OPEN

Oncogene (2016) **35,** 4321–4334

www.nature.com/onc

ORIGINAL ARTICLE

SFRP2 augments WNT16B signaling to promote therapeutic resistance in the damaged tumor microenvironment

Y Sun[1,2,3], D Zhu[4], F Chen[1], M Qian[1], H Wei[5], W Chen[5] and J Xu[4]

Most tumors initially respond to cytotoxic treatments, but acquired resistance often follows. The tumor microenvironment (TME) is a major barrier to clinical success by compromising therapeutic efficacy, and pathological relevance of multiple soluble factors released by a therapeutically remodeled TME remains largely unexplored. Here we show that the secreted frizzled-related protein 2 (SFRP2), a Wnt pathway modulator, is produced by human primary fibroblasts after genotoxic treatments. SFRP2 induction is remarkable in tumor stroma, with transcription mainly modulated by the nuclear factor-κB (NF-κB) complex, a property shared by several effectors of the DNA damage secretory program. Instead of directly altering canonical Wnt signaling, SFRP2 augments β-catenin activities initiated by WNT16B, another soluble factor from DNA-damaged stroma. WNT16B recognizes cancer cell surface receptors including frizzled (FZD) 3/4/6, a process enhanced by SFRP2, coordinated by the co-receptor LRP6 but subject to abrogation by DKK1. Importantly, we found WNT16B plays a central role in promoting advanced malignancies particularly acquired resistance by counteracting cell death, an effect that can be minimized by a neutralizing antibody co-administered with classical chemotherapy. Furthermore, DNA damage-triggered expression of WNT16B is systemic, imaged by significant induction among diverse solid organs and circulation in peripheral blood, thereby holding promise as not only a TME-derived anticancer target but also a novel biomarker for clinical evaluation of treatment efficacy. Overall, our study substantiates the biological complexity and pathological implication of a therapy-activated TME, and provides the proof of principle of co-targeting tumor and the TME to prevent acquired resistance, with the aim of improving intervention outcome in an era of precision medicine.

Oncogene (2016) **35,** 4321–4334; doi:10.1038/onc.2015.494; published online 11 January 2016

INTRODUCTION

Therapeutic resistance remains a universal obstacle in clinical oncology and is a major cause of treatment failure in patients with metastatic tumors. Most regimens are designed to target neoplastic cells, but they also damage adjacent benign constituents in the tumor microenvironment (TME), a phenomenon understood as the off-target effect of anticancer agents. Stromal cells surrounding the primary foci are capable of generating signals to influence tumor phenotypes, thereby displaying the capacity to modify all facets of disease evolution.[1] DNA damage to fibroblasts in the TME promotes synthesis and secretion of soluble factors that enable cancer cells to survive cytotoxicity and exacerbate patient pathophysiology.[2] Thus, effective targeting the treatment-elicited response of the TME holds the potential to weaken or abolish therapeutic resistance resulting from anticancer therapies *per se*. To this end, studies to corroborate the significance of a damaged TME to tumor progression while providing new opportunities for early therapeutic intervention against cancer resistance development, so far stand out with salient and paramount priority.

Advances in TME biology identified that WNT16B is an important stroma-derived factor under the pressure of chemotherapy, as it dramatically modulates cancer sensitivity.[3] As an effector of the DNA damage secretory program (DDSP) activated by treatment-delivered genotoxicity, WNT16B is upregulated in the stroma of solid tumors including but not limited to prostate, breast and ovarian malignancies.[4] Mechanistically, the nuclear factor-κB (NF-κB) complex acts as a key signaling node that mediates expression of multiple DDSP factors in the post-treatment stage, and DNA damage response signaling ultimately culminates in a phenotype characterized by persistent senescence and robust secretion that creates prosurvival, proangiogenic and proinflammatory TME niches.[5] Besides WNT16B, the DDSP effector pool covers interleukin (IL)-6, IL-8, hepatocyte growth factor (HGF), serine peptidase inhibitor Kazal type 1 (SPINK1), amphiregulin (AREG) and others that can promote adverse tumor phenotypes, particularly cancer cell repopulation and treatment resistance.[4] A detailed understanding of these paracrine signals triggered by genotoxicity provides an ideal platform for designing combinatorial strategies that simultaneously control malignant cells and the TME, in a scenario where both parts subject to the stress dynamics exerted by the antineoplastic regimens.

Members of Wnt superfamily have broad implications in embryogenesis, homeostasis and multiple pathologies.[6] Although insightful appreciation of Wnt proteins has emerged from several systems particularly human studies; therapeutic agents specifically targeting Wnt pathways have only recently entered clinical trials without reaching FDA approval.[7] In more recent work, we noticed

[1]Key Laboratory of Stem Cell Biology, Institute of Health Sciences, Shanghai Institutes for Biological Sciences (SIBS), Chinese Academy of Sciences (CAS) and Shanghai Jiaotong University School of Medicine (SJTUSM), Shanghai, China; [2]Collaborative Innovation Center of Systems Biomedicine, Shanghai Jiaotong University School of Medicine, Shanghai, China; [3]Department of Medicine and VAPSHCS, University of Washington, Seattle, WA, USA; [4]Department of General Surgery, Zhongshan Hospital, Fudan University, Shanghai, China and [5]Department of Pharmacology, Changzheng Hospital, Second Military Medical University, Shanghai, China. Correspondence: Professor Y Sun, Key Laboratory of Stem Cell Biology, Institute of Health Sciences, Shanghai Institutes for Biological Sciences (SIBS), Chinese Academy of Sciences (CAS) and Shanghai Jiaotong University School of Medicine (SJTUSM), 320 Yueyang Road, Shanghai 200031, China.
E-mail: sunyu@sibs.ac.cn
Received 4 July 2015; revised 20 November 2015; accepted 30 November 2015; published online 11 January 2016

SFRP2, a Wnt signaling regulator, was among the top list of DDSP hallmark effectors as revealed by bioinformatic analysis of human fibroblast-derived extracellular proteins after DNA damage.[4] Though frequently reported as a canonical Wnt pathway inhibitor, SFRP2 is positively correlated with malignant progression of angiosarcoma and breast tumors by inducing angiogenesis via activation of the calcineurin/NFATc3 pathway.[8] SFRP2 clearance with a monoclonal antibody inhibits activation of β-catenin and NFATc3, making this factor a novel therapeutic target for a subset of tumor types.[9] In addition, SFRP2 promotes epithelial cell transformation and induces resistance to apoptosis by increasing cell adhesion to the extracellular matrix in breast tumor, while preventing cell death in hypertrophic scar through interactions with transcription factors including Slug.[10,11] However, functional roles of SFRP2 in the settings of treatment-damaged TME remain elusive. In this study, we defined the expression mechanism of SFRP2 in primary fibroblasts, determined the biological implications of such a DDSP factor in changes occurring in tumors under treatment conditions, and explored potential interventions to circumvent the pathological impact of major soluble effectors that are critical to resistance acquired from the damaged TME, with an aim of improving therapeutic indexes in clinical oncology.

RESULTS

SFRP2 expression is inducible by genotoxicity in stroma of solid tumors

Anticancer agents cause significant cell perturbations including DNA damage, and promote tumor regression by activating apoptosis, autophagy and senescence programs. To assess the damage responses of human benign stromal cells comprising the TME, we focused on a primary prostate fibroblast line PSC27, an optimized *in vitro* cell model for tumor–stroma interaction studies.[4] Following treatments with hydrogen peroxide (H_2O_2), bleomycin or ionizing radiation (RAD), each generating remarkable DNA strand breaks in the nuclei, SFRP2 transcript was significantly upregulated in PSC27 cells with an average of 25-fold, evidence of SRFP2 overexpression in stroma on genotoxic stress (Figure 1a).

To extend the finding to more general clinical settings of prostate cancer (PCa), we examined SFRP2 induction with additional drugs including mitoxantrone (MIT) and satraplatin (SAT), two genotoxic agents frequently administered to PCa patients as components of a second-line chemotherapy.[12–14] In addition, similar treatments were performed with the human breast fibroblast line HBF1203.[4] Interestingly, SFRP2 induction was consistently observed in fibroblasts derived from both the prostate (PSC27, Figures 1b–d) and the breast (HBF1203, Supplementary Figure S1), indicating that SFRP2 expression is not restricted to certain genotoxic drug or specific organ, but universal to multiple forms of DNA damaging agents and diverse types of tissues. Encoded as a soluble factor by the DDSP program, SFRP2 was secreted into the conditioned media (CM) on treatment-provoked biosynthesis in the fibroblast cytoplasm (Figures 1c and d). In contrast to the acute response of DNA-damaged fibroblasts (usually referred to the first 24–72 h after treatment), SFRP2 upregulation was more readily detectable $\geqslant 1$ week later, an expression pattern that was indeed common for most of other secreted factors on the DDSP top list, including MMP1, WNT16B, SPINK1, MMP3, IL-8 and EREG (Figure 1e).

As previous studies reported that SFRP2 is overexpressed in the vasculature of 85% human breast cancer patients,[15] we asked whether its induction on DNA damage is general in the tumor foci or specific to some cell subpopulations, including the well-characterized lines derived from the primary or metastatic sites. Treatments to PSC27 and several typical PCa epithelial lines with RAD, MIT or SAT demonstrated that SFRP2 is more inducible in fibroblasts rather than in epithelial cells which only had minor responses, even when they received the same dose of cytotoxicity per agent (Figures 2a and b).

We recently reported that the expression of another DDSP factor, WNT16B, a human Wnt family member, arises from tumor-adjacent stroma on chemotherapy but functions as a paracrine molecule in the TME to alter multiple epithelial phenotypes.[4] As an interesting point, the DDSP is not hormone dependent, but rather relies on signals delivered by DNA damage or genotoxic stress indeed. In this study, therefore, we chose to compare the expression levels of SFRP2 in a cohort of patients diagnosed with colorectal cancer (CRC, representative of solid tumors harboring typical TMEs) between pre- and post-chemotherapy by analyzing several cell subpopulations acquired by laser capture microdissection. Data showed that SFRP2 transcripts increased remarkably in stromal cells ($P < 0.01$) but not in epithelial compartments regardless of malignancy ($P > 0.05$) (Figure 2c). As supporting evidence, results from immunohistochemistry staining of clinical specimens confirmed distinct SFRP2 expression, which was clearly more intensive in the surrounding stroma of tumor foci from patients who underwent neoadjuvant chemotherapy (Figure 2d). Echoing WNT16B induction which also displayed a stroma-specific pattern on the sequential sections from same patients (Figure 2d), our data implied that special regulatory mechanism of SFRP2 in the resident non-epithelial cells is operative. Pathological assessment of WNT16B and SFRP2 disclosed that both factors were significantly upregulated in the periglandular stroma, with the expression positively correlated (Figures 2e–g). Of note, higher expression of each protein is associated with poor clinical outcome of the CRC population (Supplementary Figure S2). Although both SFRP2 and WNT16B appear to be synthesized more readily in stroma of patients after chemotherapy, the underlying rationale remains unclear and deserves continued studies.

NF-κB complex mediates SFRP2 expression on genotoxicity-induced stress

Chemotherapy causes cellular senescence, and emerging data pinpoint NF-κB signaling as the major pathway that modulates the DDSP or forms a senescence-associated secretory phenotype, terms sharing diverse similarities.[16,17] Further, enhanced NF-κB transcriptional activity and IL-6/IL-8 secretion are among the typical markers of the secretory phenotype formed in DNA damage settings.[18] We asked whether genotoxicity-induced SFRP2 expression occurs through transcriptional regulation by the NF-κB complex. Bioinformatics identified multiple NF-κB-binding motifs in the SFRP2 approximal promoter region and *in vitro* reporter assays validated their functional relevance through a series of promoter-incorporated constructs and single-site mutagenesis (Figure 3a). It was evident that MIT, RAD or the tumor necrosis factor α, well-known NF-κB inducers, significantly promoted SFRP2 reporter activity (Figures 3a and b). Indeed, a handful of *bona fide* NF-κB-binding sites (p1–p4) exist in SFRP2 promoter as revealed by antibody-specific chromatin immunoprecipitation (ChIP) assays; data substantiated by positive controls encompassing promoter regions of typical DDSP factors including WNT16B and IL-8 (Figure 3c). The presence of multiple NF-κB-binding sites in SFRP2 promoter implies functional involvement of this transcription complex in regulating SFRP2 expression after genotoxic stress. In supporting experiments, we applied a PSC27 subline that stably expresses a mutant nuclear factor of κ light polypeptide gene enhancer in B cells inhibitor α (IκBα) ($PSC27^{IκBα}$), which blocks IκB kinase (IKK)-initiated ubiquitin-dependent IκBα degradation and thus attenuates NF-κB signaling (Supplementary Figure S3a).[4] On treatment with DNA damaging agents including bleomycin, SAT or RAD, NF-κB translocated to the nucleus with remarkably enhanced reporter activity (~10^3-fold), accompanied

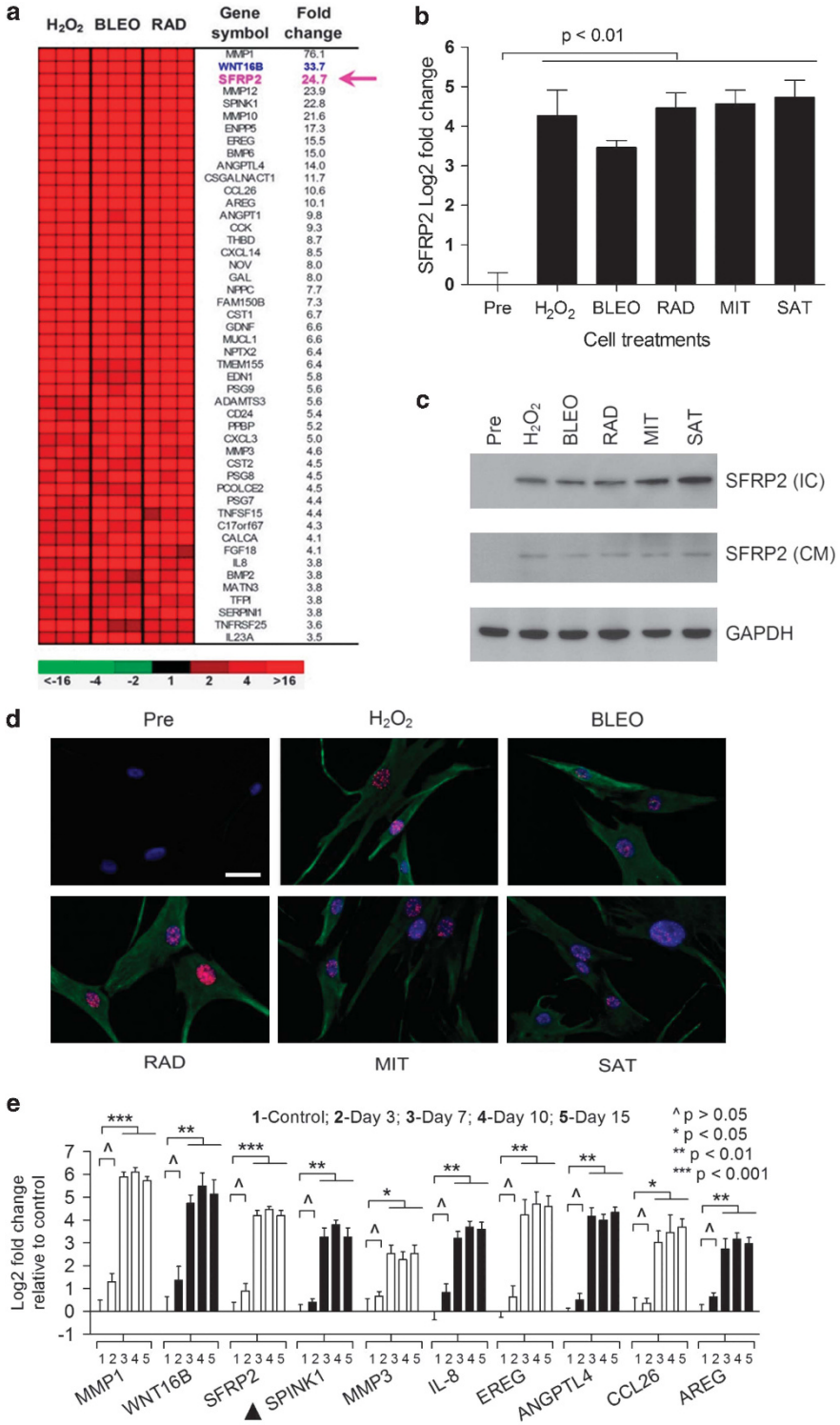

Figure 1. SFRP2 expression is induced in primary prostate fibroblasts by genotoxic agents. (**a**) Genome-wide expression microarray analysis of PSC27. Cells were exposed to H_2O_2, bleomycin (BLEO) or γ-irradiation (RAD) in culture, and compared with pre-treated cells. WNT16B and SFRP2 are highlighted in colors, image adapted from ref. 4 with permission from Nature Medicine, copyright 2012. (**b**) Ten days after treatments, cells were collected for SFRP2 expression assay by quantitative reverse transcription–PCR (qRT–PCR). Two additional genotoxic agents (mitoxantrone, MIT; satraplatin, SAT) were used, as well. (**c**) Immunoblot analysis of SFRP2 expression in the lysates (IC) or conditioned media (CM) of PSC27, GAPDH as a loading control. (**d**) Immunofluorescence (IF) staining with antibodies against SFRP2 (green), γ-H2AX (red) and DAPI (nuclei, blue). Scale bar, 15 μm. (**e**) Transcript expression of typical DDSP factors in a time course after DNA damage treatment. Cell lysates were collected at day 3, 7, 10 and 15, respectively, followed by qRT–PCR assays. Signals per factor normalized to the untreated (or pre-treatment). Data are representative of three independent experiments, with *P*-values indicated. ***$P < 0.001$.

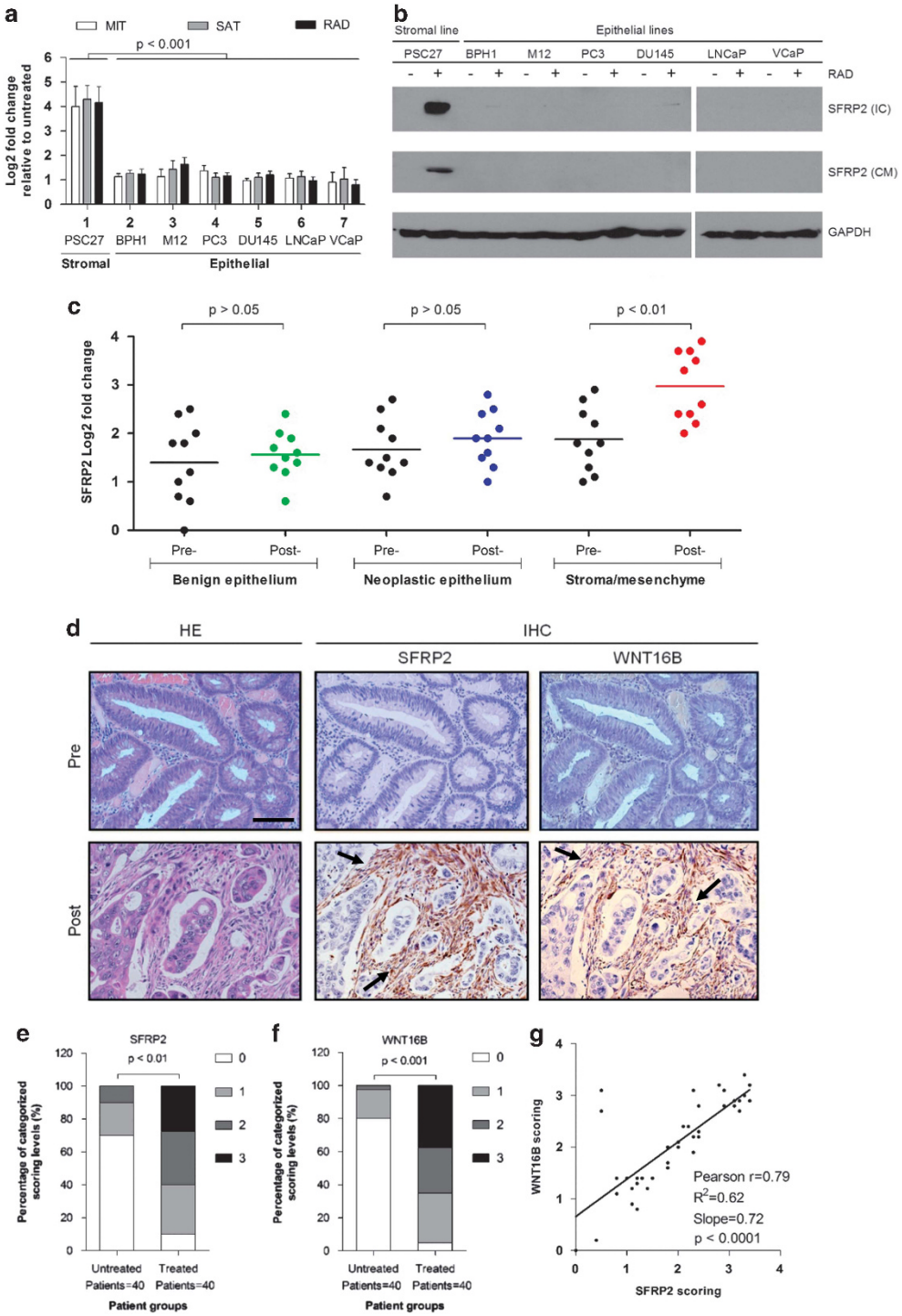

Figure 2. SFRP2 is differentially expressed between stromal and epithelial cells in response to DNA damage. (**a**) Measurement of SFRP2 transcription in prostate fibroblasts and epithelial cells after genotoxic treatments (MIT, SAT and RAD), data normalized to untreated controls per line. (**b**) Protein-level examination with samples collected from cell lines used in **a**. IC and CM samples of each line were collected ~ 10 days after γ-irradiation treatment, GAPDH as a loading control. (**c**) Expression profiling of SFRP2 in distinct cell subpopulations separately isolated by laser capture microdissection from OCT-embedded tissue specimens of human CRC patients who either received direct surgery or underwent neoadjuvant chemotherapy before surgery. Data normalized to the lowest ΔCT in the pre-treatment group. Pre-, Pre-chemotherapy; Post-, Post-chemotherapy. Each data point represents an individual patient; $n = 10$. (**d**) Representative HE and IHC staining images of sequential sections from human CRC patient specimens analyzed in **c**. Left column, HE staining; central and right columns, IHC staining. Anti-SFRP2 and anti-WNT16B were applied to tissues to probe the expression of designated antigens, respectively. Scale bar, 150 μm. Black arrows, stroma. (**e**) Pathological assessment of SFRP2 stromal expression in CRC patient tissues. For either pre- or post-treatment group, $n = 40$. Patients were assigned to four categories per IHC staining intensity. 0, no expression; 1, faint expression; 2, moderate expression; 3, strong expression. $P < 0.01$ by ANOVA. (**f**) IHC evaluation of WNT16B stromal expression in the same CRC patient cohort. (**g**) Co-expression of SFRP2 and WNT16B in stroma, corresponding R^2 represents a best fit linear regression with Pearson correlation analysis.

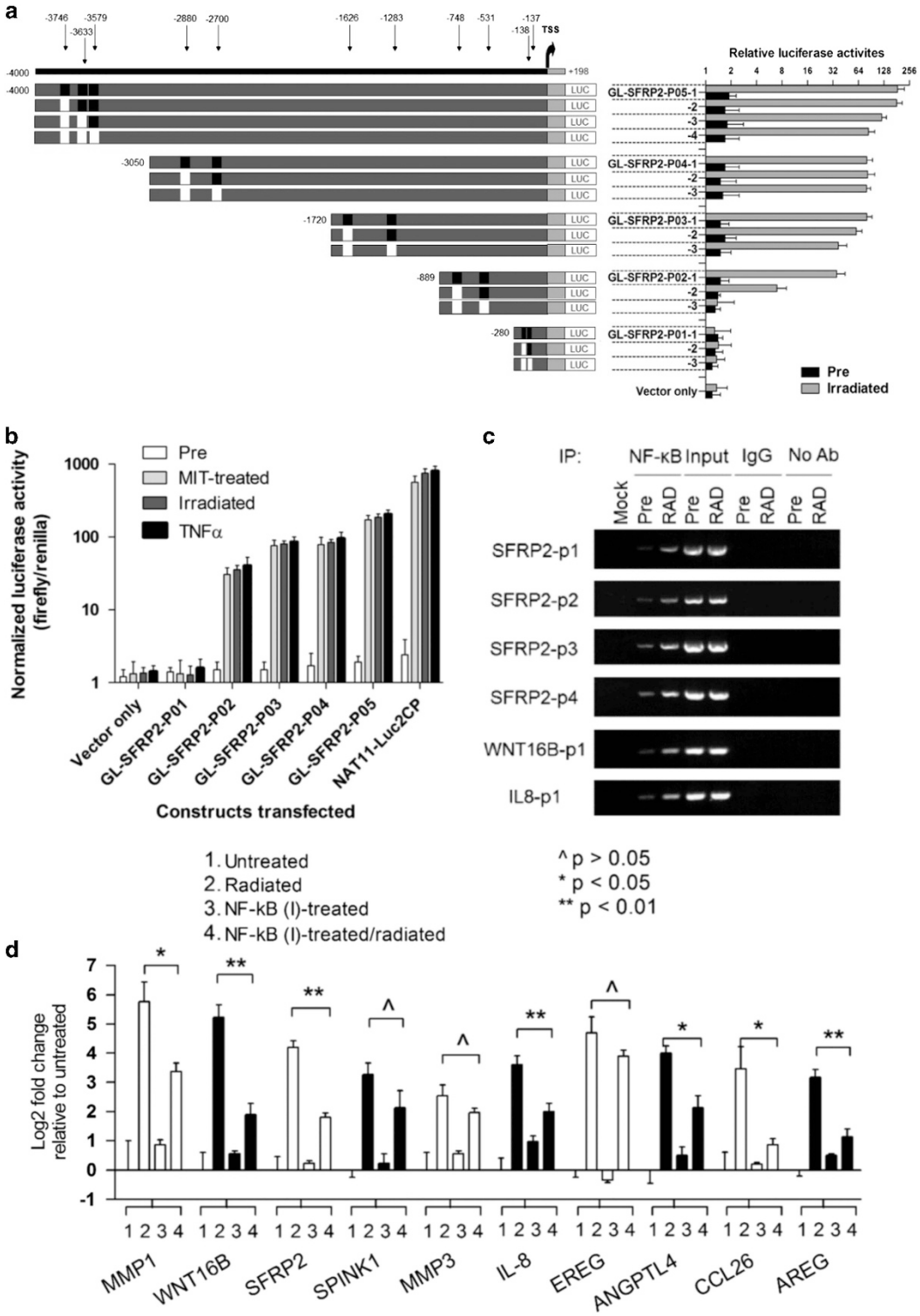

Figure 3. Genotoxic stress induces SFRP2 expression through functional activation of the NF-κB complex. (**a**) Determination of NF-κB regulatory regions in SFRP2 approximal promoter by segmental cloning and site-directed mutagenesis. Left, promoter constructs for each of the 11 putative NF-κB-binding sites in the promoter region, denoted by +198 through − 4000 bp upstream of the transcription start site (TSS). Black boxes, wild-type sequence; White boxes, mutated NF-κB-binding sites. Right, corresponding SFRP2 promoter activity with and without γ-irradiation in PSC27 cells, measured as luciferase signals. (**b**) NF-κB promoter reporter assays by comparing genotoxic insults (MIT, γ-irradiation) and biochemical stress (20 ng/ml TNF-α) to fibroblasts. The construct NAT11-Luc2CP was applied as an NF-κB promoter-positive control. (**c**) Chromatin immunoprecipitation (ChIP) assays. PCR reaction products from mock (no DNA loading), NF-κB immunoprecipitation, input total DNA and no antibody (Ab) control before treatment (Pre) and after irradiation (RAD). For PCR reactions, p1, p2, p3 and p4 primer pairs were used to amplify putative NF-κB-binding regions in SFRP2 promoter; WNT16B and IL-8 promoter assayed as controls. (**d**) Assessment of DDSP hallmark factor expression. Cells were either directly exposed to RAD or treated by the NF-κB inhibitor Bay 11-7082 at 5 μM before damage.

by increased WNT16B and IL-8 expression (Supplementary Figures S3b and c).

However, in the presence of IκBα mutant or a chemical inhibitor of NF-κB activity, Bay 11-7082, stress-associated responses were remarkably attenuated (Supplementary Figures S3c and d). Of note, PSC27 cells with disabled NF-κB signaling showed a significantly reduced SFRP2 expression after genotoxic treatments (Figure 3d). Among diverse DDSP factors overexpressed in damaged fibroblasts, many exhibited NF-κB-dependent biosynthesis including MMP1, WNT16B, IL-8 and ANGPTL4, while others like SPINK1, MMP3 and ERG did not, implying the biological complexity of DDSP signaling network, which seems to involve multiple regulatory pathways with each responsible for production of a subset of DDSP-encoded effectors.[2]

Functional implication of SFRP2 and coordinating activities of LRP6 in WNT16B signaling

Human SFRPs constitute a family of five conserved proteins that have broad implications in embryonic development and pathological conditions including tumorigenesis. Some studies suggested that SFRP2 inhibits the Wnt/β-catenin pathway thus acting as a tumor suppressor.[19,20] To the contrary, several reports claimed that SFRP2 induces tumor growth on production in certain malignancies including glioma and renal cancer by activating canonical Wnt signaling,[21,22] or stimulates angiogenesis via a calcineurin/NFAT as non-canonical Wnt transduction in breast cancer.[8,15] On WNT16B-mediated activation of canonical pathway, β-catenin is stabilized in the cytoplasm followed by nuclear translocation and subsequent enhancement of TCF/LEF signals.[4] To determine effects generated by SFRP2, we first chose to eliminate SFRP2 via gene-specific shRNAs (Supplementary Figure S4a). The transcriptional activation of TCF/LEF-downstream factors was promoted by CM from damaged fibroblasts (PSC27-RAD), an action mainly mediated by WNT16B but abrogated on WNT16B knockdown as evidenced by TCF/LEF reporter assays ($P < 0.05$) (Figure 4a). When the CM from a PSC27 subline overexpressing SFRP2 (PSC27-SFRP2) (Supplementary Figure S4b) was applied to culture PC3 cells, TCF/LEF-dependent reporter activity remained unchanged, implying SFRP2 alone did not activate this pathway (Figure 4a). However, when SFRP2 and WNT16B were co-expressed in fibroblasts (PSC27-WNT16B-SFRP2),

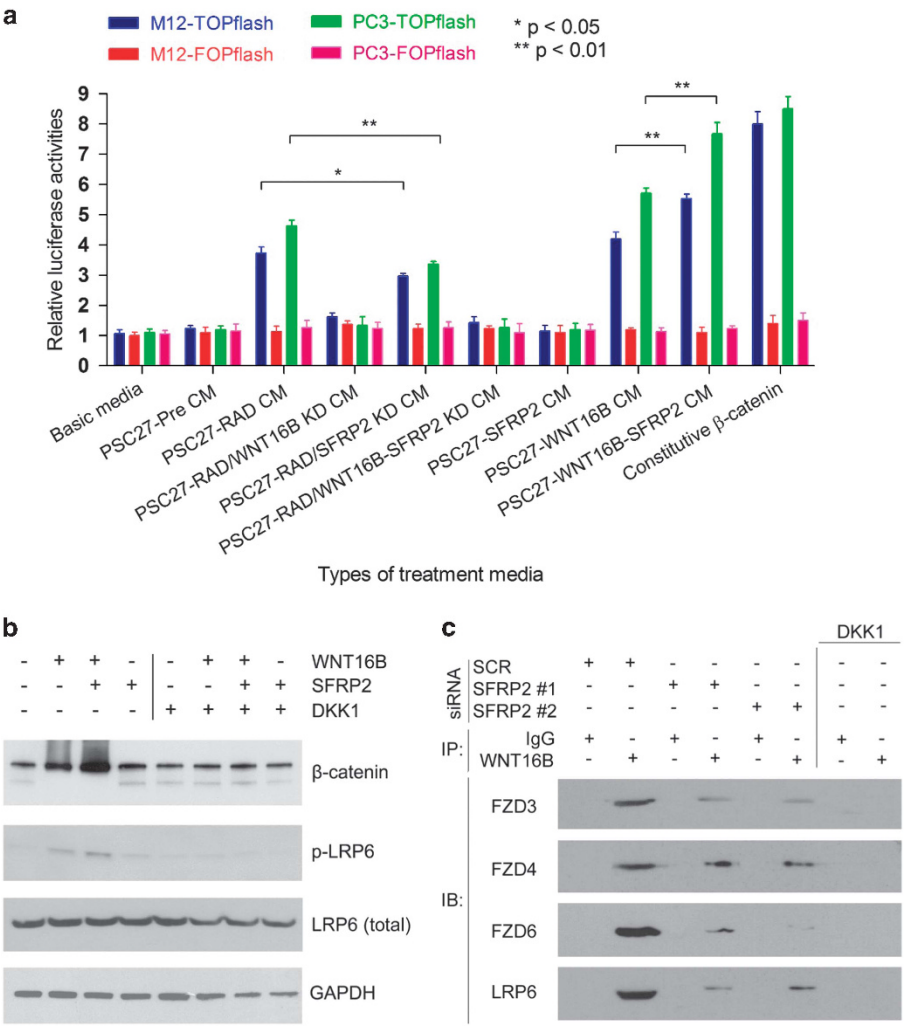

Figure 4. Activation of Wnt/β-catenin signaling mediated by WNT16B and enhanced by SFRP2. (**a**) Cell-based assay of canonical Wnt pathway activities through a TCF/LEF luciferase reporter system composed of the TOPflash and control FOPflash constructs. (**b**) Immunoblot analysis of biological effects generated by fibroblast-derived WNT16B and SFRP2 on PC3 cells under culture conditions. (**c**) Molecular associations between FZD 3/4/6, LRP6 and WNT16B. On culture with CM from PSC27-RAD fibroblasts for 3 days, PC3 cells were lysed with extracts subject to immunoprecipitation using a monoclonal anti-WNT16B (IgG as control). Pull-down precipitates were analyzed for the presence of FZD 3/4/6, LRP6 with immunoblotting. Either small interfering RNAs (siRNAs) for SFRP2 were used to suppress expression in PSC27 cells, or DKK1 provided to PC3 cells in media to inhibit Wnt signaling. SCM, scramble siRNA.

the resulting CM caused remarkable elevation of TCF/LEF activities, with signals even higher than those of the condition when WNT16B was produced alone (PSC27-WNT16B). Moreover, immunoblots demonstrated that addition of SFRP2 further increased the amount of cytoplasmic β-catenin stabilized by paracrine WNT16B in PC3 cells (Figure 4b).

DKK1 antagonizes Wnt signaling via specifically binding to the co-receptor LRP6 thereby preventing formation of the FZD/LRP6 complex and subsequent LRP6 phosphorylation induced by GSK3β.[23] In the presence of DKK1, neither WNT16B nor SFRP2 was able to induce canonical Wnt activities, and this was accompanied by diminished LRP6 phosphorylation (Figure 4b). The data suggest that recombinant DKK1 essentially blocked WNT16B-elicited and SFRP2-augmented canonical Wnt signals, a finding validated by recent literature that DKK1 inhibits canonical Wnt pathway through interfering with access of Wnt molecules that recognize spatially adjacent β-propellers/epidermal growth factor repeat pairs on LRP6 ectodomain.[24,25]

WNT16B triggers canonical Wnt pathway and transduces signals across plasma membrane, but whether WNT16B recognizes certain Wnt receptors in addition to LRP6, remains unknown. We examined the FZD family of G-protein-coupled receptors that are constitutively expressed in PC3 cells and functionally relevant in mediating WNT16B signals. Majority of the 10 human FZDs were detectable by quantitative reverse transcription–PCR (not shown), and immunoprecipitation assays indicated the molecular association between WNT16B and FZD 3, 4 and 6 on exposure of cancer cells to PSC27-RAD CM (Figure 4c). However, when SFRP2 was genetically removed from the fibroblasts prior to DNA damage, interactions between WNT16B and its receptors were significantly weakened, implying that SFRP2 plays an important role in consolidating the association between WNT16B and the individual receptors. Surprisingly, the physical interplays between WNT16B and FZDs or LRP6 even diminished when DKK1 was applied at a concentration of 10 nM (Figure 4c), indicating a pivotal role of LRP6 in coordinating the association of WNT16B and the receptor complex.

SFRP2 augments WNT16B signaling to promote malignant phenotypes of PCa cells

The damage-responsive program DDSP comprises a wide spectrum of soluble factors with the capacity to modify the phenotypes of cancer cell populations through paracrine pathways.[16] We next sought to determine whether SFRP2 is involved in cancer progression on establishment of a fibroblast-specific secretion phenotype under genotoxic conditions. CM derived from radiated PSC27 fibroblasts (PSC27-RAD) increased proliferation by 2.7–3.3 fold, migration by 1.9–2.4 fold and invasiveness by 2.9–3.7 fold of neoplastic prostate epithelial lines (Figure 5a; Supplementary Figures S5a–c). In the absence of SFRP2, CM from damaged fibroblasts produced less effects to cancer cells with a reduction of ~10–15%, depending on the cell line. In contrast, phenotypic changes were more dramatic if WNT16B expression was suppressed, which caused a reduction of 28–35%. Interestingly, when both SFRP2 and WNT16B were eliminated from PSC27 cells, the reduction percentage of each epithelial phenotype resembled that of conditions when WNT16B was silenced alone.

To further characterize the functional involvement of stromal SFRP2 in altering cancer cell phenotypes, we applied MIT, the type II DNA topoisomerase inhibitor frequently combined with prednisone as a second-line treatment for metastatic castration-resistant PCa. Epithelial cells exposed to PSC27-RAD CM showed significantly improved survival on cytotoxic treatment (IC50, Figure 5b). In contrast to SFRP2, WNT16B conferred higher extent of protection against cell death. When both SFRP2 and WNT16B were withdrawn from the full DDSP spectrum, the consequence was similar to that caused by CM from the condition when only WNT16B was eliminated. Altogether, data derived from prostate epithelial cells strongly support that WNT16B is one of the major secreted factors that substantially promote cancer resistance, whereas functional effects of SFRP2, however, principally rely on the presence of WNT16B in the microenvironment.

To further confirm the findings and explore the feasibility to specifically target WNT16B, a critical Wnt pathway ligand produced by the stromal DDSP to promote malignancy via its paracrine activities, we purified a monoclonal WNT16B antibody obtained from a commercial source (Supplementary Figure S6a). Cell apoptosis measured 24 h after MIT exposure was markedly alleviated by CM from PSC27-RAD cells, an effect that was significantly reversed by anti-WNT16B as compared with the non-specific control IgG (Figures 5c and d). CM from damaged PSC27, representing the full fibroblast DDSP, increased the viability of PC3 cells exposed to MIT at concentrations ranging from 0.1 to 1 μM in culture, while anti-WNT16B abrogated such protection with the efficacy close to that of XAV939, a potent small molecule inhibitor of canonical Wnt pathway used as a positive control (Figure 5e).

Anti-WNT16B promotes cancer cell apoptosis *in vivo* on chemotherapy

We next interrogated whether antibody-mediated WNT16B suppression causes *in vivo* responses following genotoxic treatment to experimental animals. For this purpose, we performed SCID mice-based subrenal capsule xenografting with tissue recombination, where PC3 cells were pre-admixed with PSC27 fibroblasts at an optimized ratio of 4:1. Two weeks after transplantation when tumors showed stable intake by animals, a single dose of MIT or placebo was administered along with anti-WNT16B or IgG. Seven days after treatment, the tumors were dissected for tissue analysis with immunofluorescence staining. In contrast to placebo, MIT-associated genotoxicity triggered remarkable nuclear transportation of β-catenin in cancer cells (Figure 6a). However, co-administration with anti-WNT16B through i.p. injection significantly prevented such cytoplasm-nucleus translocation, as evidenced by confocal imaging. Compared with the non-specific IgG, anti-WNT16B markedly enhanced the number of apoptotic cells in tumor xenografts, even in the presence of PSC27 fibroblasts (Figure 6b). Statistical data indicated that DNA damage index remained unchanged when anti-WNT16B was administered to animals, but the percentage of caspase 3-positive cells increased significantly as compared with the IgG group (Figure 6c). To confirm the apoptotic responses mediated by anti-WNT16B upon chemotherapy, we made castration-based but androgen-sensitive xenografts consisting of PSC27 and VCaP, the latter an epithelial line biologically recapitulating human CRPC conditions.[26] Although the percentage of apoptotic cells increased in these tumors, delivery of anti-WNT16B repeated the results observed in PC3-bearing tumors (Figure 6d). Our data suggested that elimination of WNT16B from the damaged TME contributed to increased responses to chemotherapy, as co-targeting cancer cells and a key DDSP effector significantly improved cancer cell apoptotic index, results independent of androgen response/AR signaling activities of the prostate tumors *per se*.

Targeting WNT16B minimizes resistance acquired from the treatment-damaged while functionally activated TME

To determine the pathological influence of the treatment-remodeled TME on tumor resistance *in vivo*, we xenografted mice with PC3 and PSC27, with fibroblasts pre-exposed to radiation *in vitro* and performed a longer follow-up. Two weeks after transplantation, anti-WNT16B was administered as one-time injection. At the end of an 8-week course, tumors were dissected with volumes measured. In contrast to PSC27 control grafts (PC3+PSC27) which averaged 308 mm^3, sizes of grafts harboring

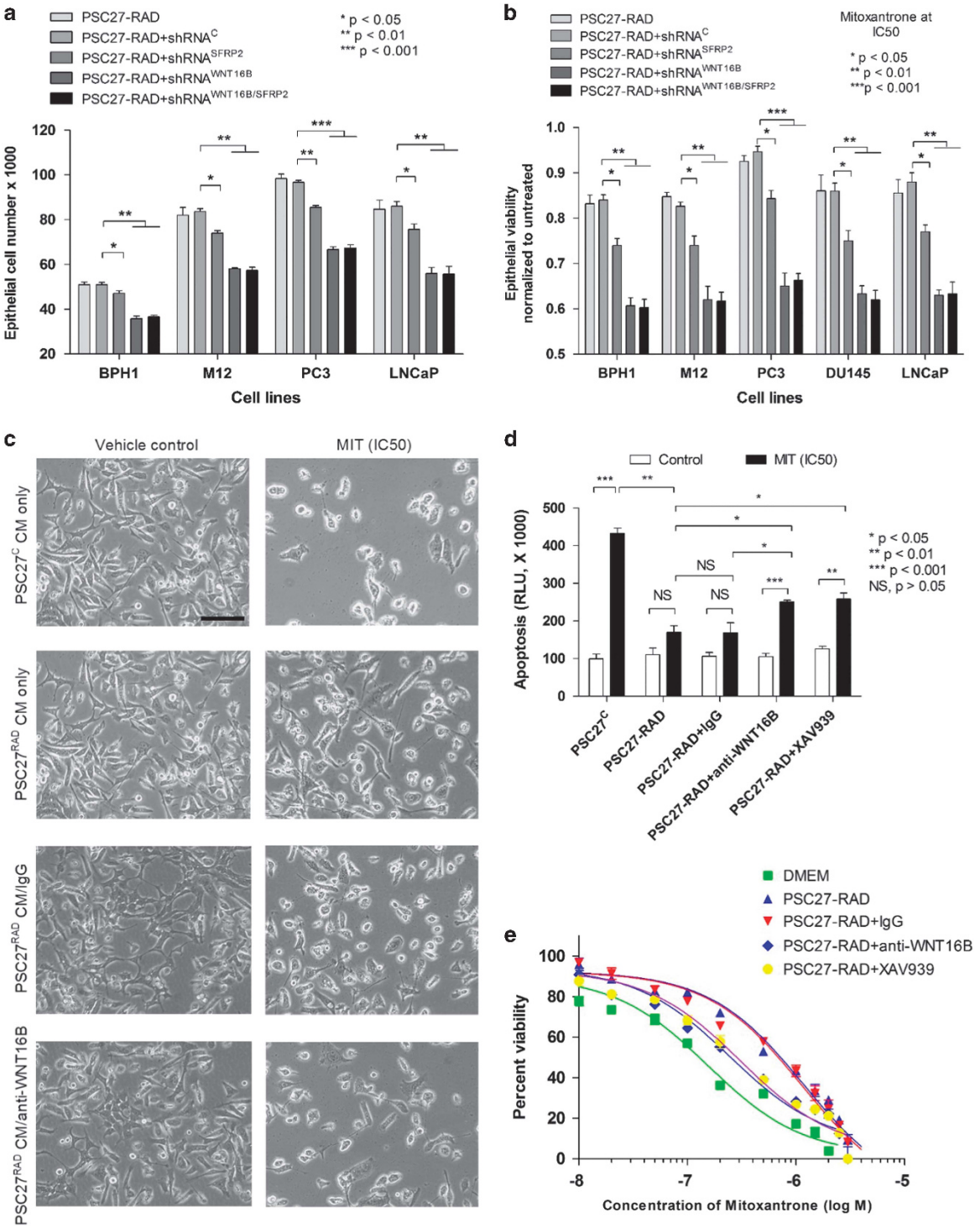

Figure 5. SFRP2 promotes PCa epithelial cell proliferation and resistance to cytotoxic chemotherapy in a WNT16B-dependent manner. (**a**) SFRP2 contributed to PC3 proliferation, an activity dependent on the presence of WNT16B. Full spectrum of fibroblast DDSP caused by γ-irradiation (PSC27-RAD) accelerated growth of PC3 cells, which was less when SFRP2 was knocked down (PSC27-RAD+shRNA^{SFRP2}) or attenuated once WNT16B was eliminated (PSC27-RAD+shRNA^{WNT16B}). (**b**) SFRP2 augmented PC3 chemoresistance. Similar to the case of **a**, functional gain was significant but relied on the existence of WNT16B in culture. (**c**) Cancer cell images by brightfield microscopy. PC3 cells were cultured with CM from different cell groups, photographed 24 h after exposure to vehicle or MIT at IC50. Scale bar, 50 μm. (**d**) Quantification of apoptosis *in vitro* by assays reporting combined activities of caspase 3 and 7 measured 24 h post exposure of PC3 cells to vehicle or MIT at IC50, with XAV939 as a positive control for Wnt pathway inhibition. RLU, relative luciferase unit. (**e**) Viability of PC3 cells across a range of MIT concentrations under conditions used in **d.** NS, not significant.

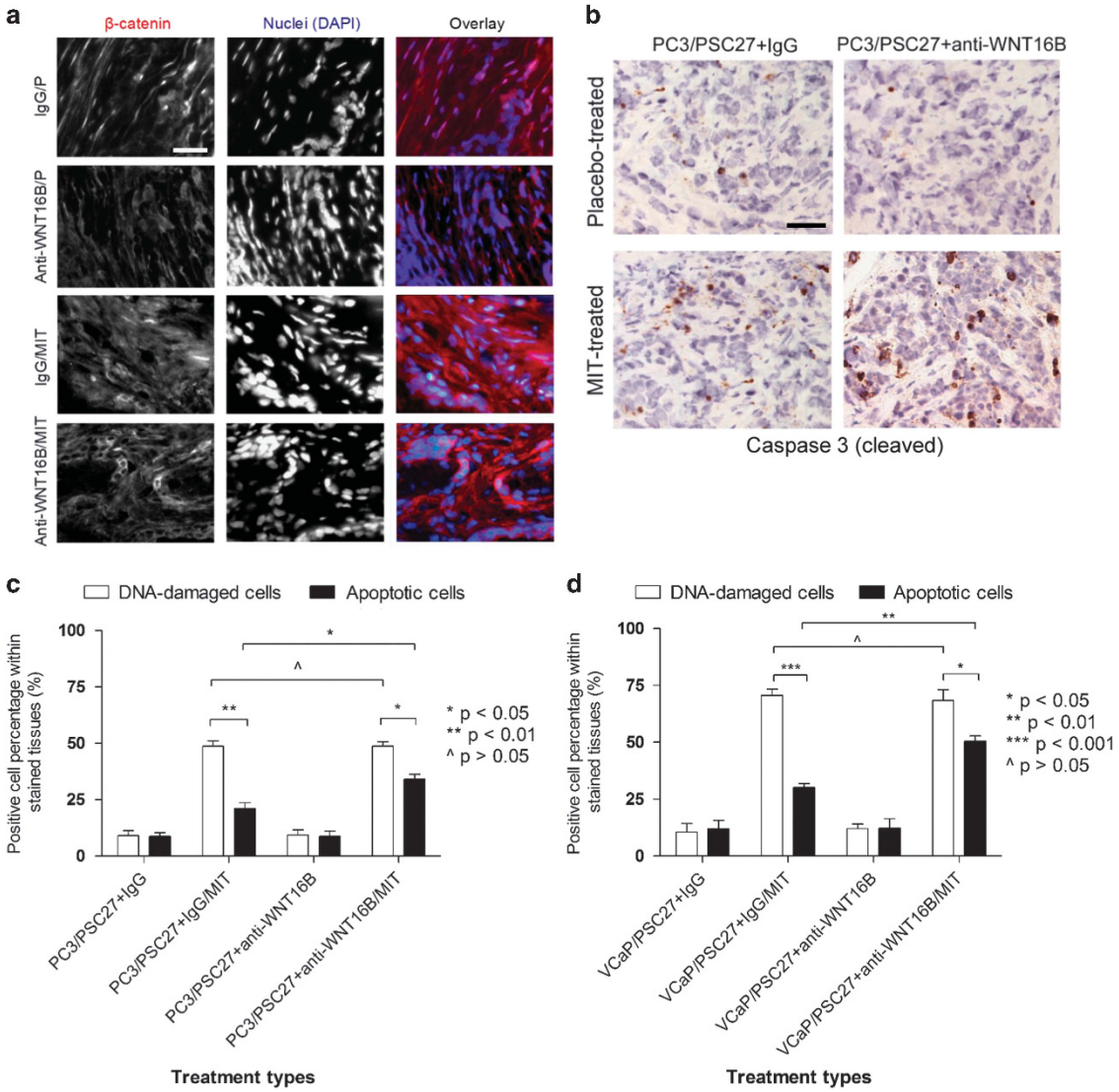

Figure 6. *In vivo* influence of anti-WNT16B to tumor survival on exposure of immunodeficient (SCID) mice to chemotherapy. (**a**) IF staining of β-catenin on tissue sections obtained from mouse xenografts comprising PC3 cells and PSC27 fibroblasts. Scale bar, 50 μm. (**b**) IHC staining of xenografts with anti-caspase 3 (cleaved). Mice were killed 7 days post treatment to evaluate acute cancer cell responses to chemotherapy *in vivo*. Scale bar, 50 μm. (**c**) Quantification of apoptosis by IHC staining against cleaved caspase 3 and of DNA damage by IF staining with anti-γH2AX after treatment with agents delivered in conditions of **a** and **b**. Values represent a minimum of 100 cells counted from each of 3–5 tumors per group. (**d**) Similar assays performed for tumor xenografts composed of PSC27 fibroblasts and VCaP cells, the latter AR positive and androgen independent.

PC3 and damaged PSC27 (PC3+PSC27-RAD) increased to 588 mm^3 (Supplementary Figure S6b). Anti-WNT16B treatment did not change the volumes of PC3+PSC27 tumors, but reduced the sizes of PC3+PSC27-RAD grafts to 430 mm^3, representing a 26.8% shrinkage ($P < 0.01$).

To more precisely simulate the physiological reality of cancer therapy in clinical settings, we generated grafts with undamaged (or native) PSC27 fibroblasts, and followed another 8-week regimen composed of three cycles of MIT given every other week starting from the beginning of the 3rd week (Figure 7a). Chemotherapy to PC3-only animals dramatically reduced tumor sizes (59.2%, $P < 0.001$), whereas anti-WNT16B did not further improve the outcome ($P = 0.18$) (Figure 7b). Although co-transplantation of PC3 cells and PSC27 fibroblasts allowed tumor size to increase remarkably (averaged at 307 mm^3), MIT treatment resulted in a prominent reversal of tumor expansion by 38.8% (to 188 mm^3) ($P < 0.001$). Surprisingly, co-administration of MIT and anti-WNT16B generated a significantly enhanced tumor regression, with a final volume averaged at 122 mm^3, which was an additional reduction of 35.1% compared with MIT treatment alone (Figures 7b and c). Similar efficacy of combinational treatment was observed in the VCaP/PSC27 group, where anti-WNT16B generated an additional shrinkage of tumors by 30.2% (Supplementary Figure S6c). To generalize the findings to alternative types of solid tumors, we applied such combinational treatments to xenografts composed of breast cancer cells MDA-MB-231 and breast fibroblasts HBF1203, with similar efficacy achieved (33.4%) (Supplementary Figure S6d).

Epithelial-to-mesenchymal transition is a typical change of cancer cell phenotype, as induced by the therapy-damaged fibroblasts to promote resistance, substantially driven by WNT16B via a paracrine action *in vitro*.[4,27] In this study, MIT-delivered cytotoxicity caused a typical epithelial-to-mesenchymal transition switch as evidenced by Immunofluorescence staining of xenograft tissues, with decreased E-cadherin expression in the cytoplasm and concurrently increased β-catenin accumulation in PC3 nuclei

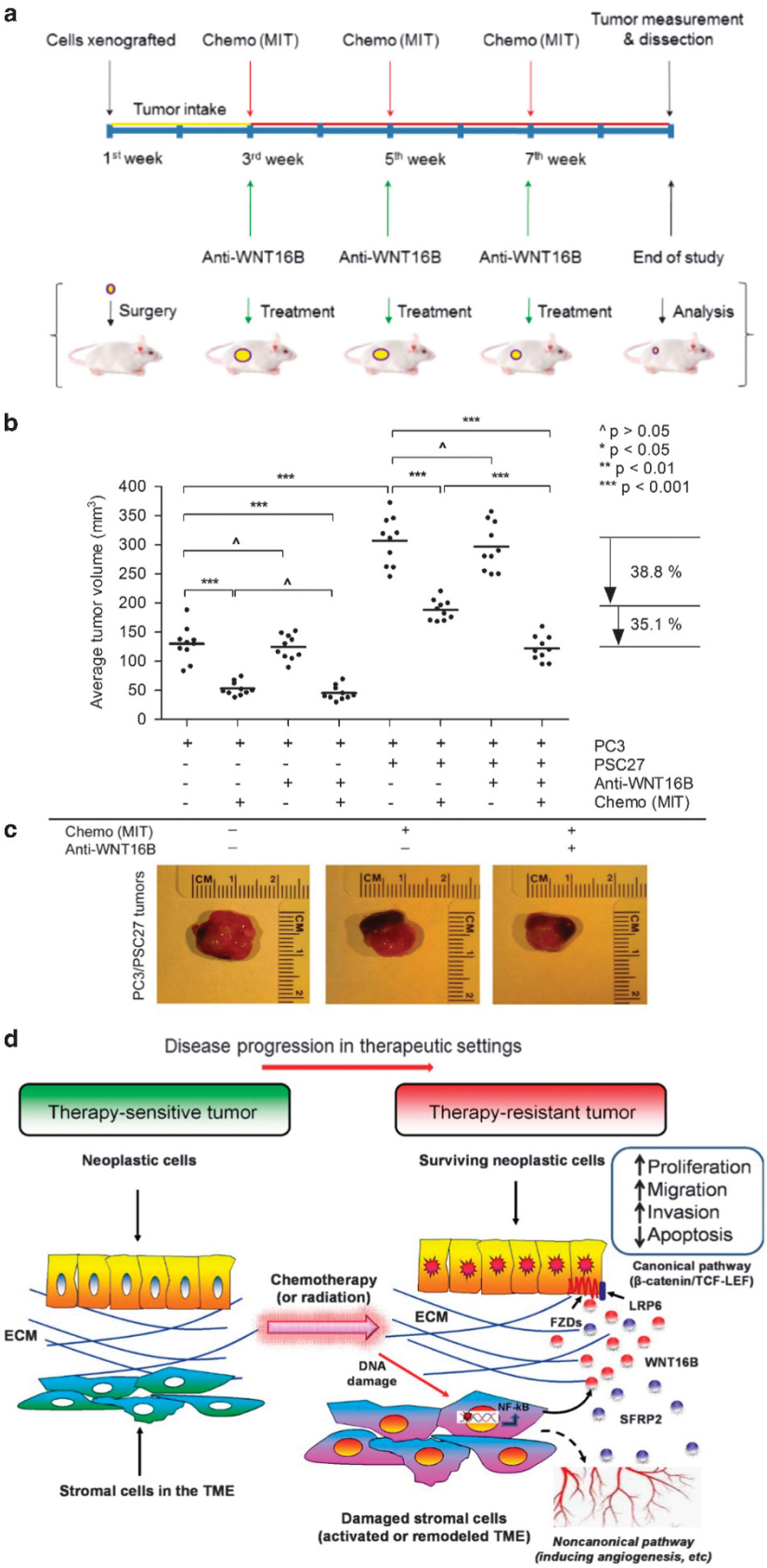

(Supplementary Figure S7a). However, anti-WNT16B, through neutralizing the specific target WNT16B in TME niches, remarkably reversed the epithelial-to-mesenchymal transition-associated tendency (Supplementary Figures S7a and b). As supporting evidence, similar changes were observed in VCaP/PSC27 and MDA-MB-231/HBF1203 tumors (not shown).

To examine the systemic consequence of chemotherapy in experimental mice that received MIT administration via i.v. infusion, we performed comprehensive analysis of several solid organs including prostate, lung, colon and circulating blood. Of note, immunoblot analysis indicated the presence of WNT16B in not only solid tissues but also the serum of treated animals, with data convincingly consolidated by enzyme-linked immunosorbent assay (ELISA) assays (Supplementary Figures S8a and b). Thus, experiments disclosed the fact that typical DDSP effectors like WNT16B generated as soluble factors by the damaged TME are indeed capable of entering circulation, which allows detection by routine biotechniques. WNT16B and other factors including IL-8 released by the microenvironment (Supplementary Figure S8b) under chemotherapy or radiation may represent novel biomarkers for clinical diagnosis to help assess therapeutic efficacy and evaluate tissue damage in the setting of anticancer therapeutics in clinical oncology.

DISCUSSION

Acquired resistance presents a major challenge to cancer therapies. To date most studies focus on cell intrinsic or autonomous mechanisms of cancer resistance arising in response to therapeutic regimens. However, mounting lines of evidence indicate that the TME confers exogenous resistance to cancer cells.[28,29] In solid tumors, the TME consists of the extracellular matrix, cancer-associated fibroblasts, endothelial cells, neuroendocrine cells, pericytes, immune and inflammatory cells, each lineage contributing to tumor heterogeneity, which is associated with altered drug responses.[30] The protection exerted by activated TME forms a refuge for cancer cell populations including cancer stem cells against cytotoxic agents, thus enabling them to evade apoptosis and develop acquired resistance as a prerequisite for disease recurrence.[31,32] The TME-mediated resistance to chemotherapy, radiation or targeted therapies has entered the spotlight of intensive investigation, and we recently identified WNT16B as an important TME-derived and treatment-induced modulator of chemotherapeutic sensitivity.[4,33] Numerous proteins are generated by cancer-adjacent stroma on therapy-caused tissue damage, and whether there are molecular interactions between these soluble factors remains unknown. In this study, we report that SFRP2, a Wnt pathway regulator, is produced by human fibroblasts that display a secretory phenotype. Importantly, SFRP2 functions as an active agonist of WNT16B, and promotes cancer resistance in the context of treatment-caused tissue damage. Our finding further highlights the biological complexity of the TME, particularly in pathological settings where the disease resistance evolves under therapeutic pressure.[34]

The canonical Wnt pathway medicated by β-catenin signaling has a crucial role in embryonic development, stem cell maintenance and tumor progression.[6] Although Wnt/β-catenin activities can be either positively or negatively correlated with patient outcomes in a cancer stage- and/or type-specific manner, WNT16B is not only as a senescence marker but a tumor promoter that exerts paracrine effects via promoting treatment resistance.[4,35] Due to the sequence homology with Wnt-binding domain of FZD receptors, SFRP2 used to be considered antagonist of canonical Wnt signaling.[20] However, experimental data suggested that SFRP2 augments the oncogenic activities of WNT16B by facilitating cancer cell proliferation, migration, invasion and more importantly, drug resistance. In fact, synergistic effects of SFRPs on Wnt signaling have been reported in several former studies, particularly that SFRP2 enhances Wnt3a-dependent phosphorylation of LRP6 and promotes β-catenin cytoplasmic stability accompanied by nuclear translocation.[36,37] Interestingly, stroma-derived SFRP2 alone neither activated β-catenin signaling nor caused cancer cell phenotypic changes, activities essentially reliant on the presence of WNT16B co-expressed from damaged fibroblasts. On mammalian cell surface, Wnt proteins recognize two types of receptors, including the serpentine receptor family of FZDs and the single-pass transmembrane receptors LRP5/6.[6] Experiments indicated phosphorylation of LRP6 in cancer cells when WNT16 was present, a reaction further enhanced by SFRP2. However, Wnt signaling was abrogated by silencing SFRP2 or treatment with DKK1, as evidenced by the diminished interactions between WNT16B and several FZDs. Since DKK proteins inhibit Wnt pathway by directly binding to the ectodomains of LRP5/6,[38] it is reasonable to speculate the functional importance of LRP6 in organizing the receptor complex that comprises both LRPs and FZDs to transduce Wnt signals, whereby LRP6 is a critical molecule to physically bridge WNT16B and FZDs. Within extracellular microenvironments, nevertheless, how SFRP2 augments WNT16 activities remains unclear; one possibility is that mutual binding of two secreted proteins may increase their individual stability, particularly in a context of protease-enriched TME milieu including multiple MMPs that are co-released by the treatment-damaged stroma (Figure 1a).

The regulation of DDSP is complicated, with mechanisms implicating DNA damage repair, chromatin remodeling by HDAC1

Figure 7. Chemotherapy resistance acquired from the damaged TME but attenuated by a WNT16B-targeting agent. (**a**) Schematic outline of the chemotherapeutic regimen applied to SCID mice on subrenal capsule implantation. Within the first 2 weeks, xenografts were allowed to settle in the capsules for sufficient intake. Administration of MIT and/or anti-WNT16B was performed on the 1st day of the 3rd, 5th and 7th week, with tumors collected at the end of 8th week. Drugging route, i.p. injection. (**b**) *In vivo* effects of MIT treatment, WNT16B targeting or combinatorial therapy. Agents MIT and anti-WNT16B were administered either alone or combined as synergistic treatment. Xenografts comprised PC3 cells admixed with PSC27 fibroblasts. Tumor volumes of PC3/PSC27C grafts were $307.0 \pm 13.17\ mm^3$, those of PC3/PSC27C +MIT $188.2 \pm 5.560\ mm^3$, and those of PC3/PSC27C+MIT+anti-WNT16B $122.2 \pm 6.728\ mm^3$ ($P < 0.001$). $n = 10$ per group. Vertical arrows between horizontal lines at margin show percentage of tumor reduction. (**c**) Representative photographic images of renal capsule-based tumors on animal dissection after specified treatments. (**d**) Mechanistic model of the pathological influence of treatment-damaged TME, which modifies drug sensitivity through the WNT16B/SFRP2 axis. DNA damage caused by anticancer agents including chemotherapy and radiation shrink the bulk of tumors, however, it also provokes a typical DDSP phenotype characterized with stromal generation of multiple soluble factors including WNT16B and SFRP2 in a cell non-autonomous manner. The NF-κB complex plays an important role in transcription of many DDSP effectors. Secretion of WNT16B into the TME niche promoted tumor growth by activating canonical Wnt pathway in cancer cells, resulting in decreased therapeutic sensitivity. Acquired resistance develops and disease progression continues under treatment pressure. SFRP2, as a co-effector, further enhances WNT16B/β-catenin activity to shape diverse malignant phenotypes particularly resistance, and formation of FZDs/LRP6 receptor complex at cancer cell surface is essential for signal transduction. In addition, SFRP2 may also be involved in non-canonical pathways, for example, inducing angiogenesis via activation of the calcineurin/NFATc3 signaling of endothelial cells, indirectly contribution to tumor evolution. Red droplets, WNT16B; blue droplets, SFRP2; serpentine lines, FZD receptors; dark blue bars, LRP6 co-receptor; red branches, neovasculature.

inhibition, IL-1α autocrine stimulation, and transcriptional activation by NF-κB and C/EBPβ.[5,39–41] Recent studies indicated p38MAPK mediates secretory phenotype development driven by NF-κB, with the regulation possibly more prominent in the early stage of DNA damage response.[42] In this study, we interrogated whether SFRP2 production is transcriptionally controlled by NF-κB after genotoxic treatment, and immunoprecipitation data revealed the presence of multiple NF-κB-binding sites in SFRP2 promoter. It is noteworthy that the NF-κB-regulated SFRP2 expression pattern resembles that of other effectors including the recently reported WNT16B, indicating a broad implication of this transcriptional machinery in modulating DDSP program. Although transcriptional signals persisted even after effective blockage of NF-κB activation, a phenomenon implying engagement of other molecular pathways including C/EBPβ and/or AP-1 on genotoxic treatment,[43] the NF-κB complex emerges as a master regulator of multiple DDSP factors including but not limited to WNT16B, IL-6 and IL-8.[27] However, given the high toxicity of general NF-κB suppression to diverse cell types, caution should be exercised to prevent severe side effects when selecting this complex as a therapeutic target, whereas alternative signaling nodes may be considered with higher priority such as the mammalian target of rapamycin.[44] On the other hand, of note, SFRP2 expression exhibits cell lineage specificity, with fibroblasts of higher induction potential in genotoxic settings. The mechanisms underlying robust biosynthesis in stroma contrasting relatively marginal production of SFRP2 in cancer cells on genotoxic stress remain elusive, but SFRP2 hypermethylation is a common event in multiple malignancies including PCa, and SFRP2 tends to be gradually lost from benign to malignant prostate glands as revealed by previous tissue microarray analysis.[45,46]

Antibodies that specifically target oncoproteins, cytokines or their associated signaling in the TME directly inhibit tumor progression and represent an effective option for cancer treatment.[47,48] We applied the purified monoclonal antibody against WNT16B, a TME-generated unique Wnt molecule that confers acquired resistance to cancer, and observed considerably improved preclinical outcome in restraining tumor survival. PCa recurrence involves continued growth of neoplastic epithelial cells, as the androgen-dependent disease progresses to CRPC following initial androgen-deprivation therapy. Despite recent success with anti-androgens including abiraterone and enzalutamide (MDV3100), durable responses are limited and acquired resistance develops. Alternative treatments including the second-line chemotherapy usually involving MIT, SAT or docetaxel, are thus essential to control tumor growth in patients who have failed androgen-deprivation therapy. However, acquired resistance to chemotherapy remains the major limitation of therapeutic efficacy, and interactions between tumors and their surrounding microenvironments cause disease exacerbation in PCa patients. Besides SFRP2 and WNT16B, typical DDSP factors including IL-6, IL-8, EREG and AREG may activate pathways associated with the proliferation and survival of PCa cells, therefore also linked with resistance to chemotherapy independent of the AR axis.[12] Altogether, this is a first report documenting that stroma-derived SFRP2 interacts with a co-released DDSP factor to activate the canonical Wnt pathway thereby promoting chemotherapy resistance (Figure 7d), and the effects can be eliminated by antibody-mediated treatment on combination with conventional chemotherapy. It is increasingly evident that individual compartments of the TME do not stay as quiet bystanders, but significantly influence tumor initiation, growth, metastasis, and more importantly, therapeutic response.[49] To this end, we discovered that SFRP2 augments WNT16B signaling to significantly confer therapeutic resistance. Cancer is not a solo production but rather an ensemble performance, as supported by the fact that benign cells in the surrounding milieu of cancer cells actively facilitate the malignant progression, even under therapeutic conditions. In this study, we determined the expression pattern of SFRP2 and disclosed its influence on WNT16B-associated cancer activities, exemplifying the complex dynamics of soluble factors in the TME where cancer cells are subject to treatment selection pressure.

Our study provides a novel strategy for targeting cancer cells while effectively manipulating the TME components to achieve optimal therapeutic indexes, and presents a group of emerging biomarkers that may be exploited for pathological surveillance of patient TME activity and practical targeting as an essential part of well-tuned anticancer interventions. In nature, our findings have broad implications for multiple tumor types, and open new avenues to improve therapeutic outcome by demonstrating the prominent translational value of targeting a therapeutically activated but functionally deleterious TME in the upcoming era of precision oncology.

MATERIALS AND METHODS

Cell lines and treatments

Normal human primary prostate fibroblast line PSC27, breast fibroblast line HBF1203, prostatic epithelial lines BPH1, M12, DU145, PC3, LNCaP, VCaP and breast cancer cell line MDA-MB-231 (ATCC, Manassas, VA, USA) were cultured as previously described.[4] For DNA damage, fibroblasts were grown until 80% confluent and treated with individual agents at optimized concentrations as reported previously.[4]

Constructs and lentivirus

Human SFRP2 full length complementary DNA cloned between *Rsr*II and *Not*I in the vector pCMV6-AC (Origene, Rockville, MD, USA) was digested with *Bam*HI and *Xho*I, then subcloned into pLenti-Puro. WNT16B complementary DNA was cloned in pLenti-CMV/2-Puro-DEST as described formerly.[4] Expression constructs and shRNAs to SFRP2 and WNT16B (Thermo Scientific, Waltham, MA, USA) were packaged into lentivirus, individually.

Immunofluorescence analysis

Primary mouse monoclonal anti-phospho-Histone H2A.X (Ser139) (Cat. No. 05-636-I, clone JBW301, Millipore, Billerica, MA, USA) and rabbit polyclonal anti-SFRP2 (Cat. No. sc-13940, Santa Cruz, Dallas, TX, USA) were applied for cell staining. For human tissue sections, mouse anti-SFRP2 (Cat. No. MABC539, clone 80.8.6, Millipore) and mouse anti-WNT16B (Cat. No. Cat. No. 552595, clone F4-1582, BD Pharmingen, San Diego, CA, USA) were used. For animals, antibodies against E-cadherin (Cat. No. ab1416, clone HECD-1, abcam, Pudong, Shanghai, China) and β-catenin (Cat. No. ab22656, clone 12F7, abcam) were employed.

In vitro cell assays

Confluent PSC27 fibroblasts were incubated for 3 days in DMEM+0.5% FBS, with supernatant harvested as fibroblast-derived CM. Epithelial cells were treated with CM, followed by *in vitro* assays. For canonical Wnt pathway blockage, DKK1 was added to a final concentration of 10 nM. For chemoresistance, epithelial cells were cultured with fibroblast CM while receiving MIT near individual cell line's IC_{50}.

Expression microarray

Whole genome Agilent microarray analysis was performed as described previously.[4]

Patient specimen acquisition and analysis

Administration of fluorodeoxyuridine and oxaliplatin was performed as preoperative hepatic and regional arterial chemotherapy (PHRAC) to patients with stage II (T3–4, N0, M0) or stage III (T0–4, N1–2, M0) CRC based on a thorough preoperative evaluation. Eligible patients of < 75 years with histologically proven adenocarcinoma of the colon or rectum, no severe major organ dysfunction, were randomly assigned to receive either PHRAC or surgery alone (40 patients/group). Written informed consent was provided by all patients. Randomized control trials protocol was approved by the Institutional Review Board of Fudan University School of Medicine, with methods carried out in accordance with the approved guidelines.

Data regarding tumor size, histologic type, tumor penetration, lymph node metastasis and pathologic TNM disease stage were obtained from the pathologic records (Supplementary Table S1), with chemotherapy performed as previously reported.[50] OCT-frozen specimens were processed for laser capture microdissection, with formalin-fixed paraffin-embedded sections subject to histological assessment. For gene expression, stromal compartments (associated with tumor foci)/benign epithelium/cancer epithelium were separately isolated from patient-matched tumor biopsies before and after chemotherapy using an Arcturus (Veritas Microdissection, Waltham, MA, USA) laser capture microscope following the criteria defined formerly.[7]

NF-κB regulation assays

Genetic blockage of NF-κB nuclear translocation was performed as described previously,[4] with chemical inhibition achieved with a small molecule inhibitor Bay 11-7082 (Selleck, Huangpu, Shanghai, China) at 5 μM in culture.

SFRP2 promoter analysis and ChIP assays

A 4000-bp region immediately upstream of the human SFRP2 gene was analyzed for core NF-κB-binding sites. After ChIP assays the immediate 5′ upstream sequences containing putative NF-κB-binding elements were amplified from human genomic DNA. Plasmids containing multiple mutant NF-κB-binding site(s) were generated from the reporter constructs by site-directed mutagenesis (Strategene, Santa Clara, CA, USA).

Purification, refolding and validation of anti-WNT16B

Mouse anti-human WNT16B monoclonal antibody was purified by affinity chromatography using a Sephadex G25 gel filtration column (Madison, WI, USA). After one-step chromatographic purification in denaturing conditions, dialysis was followed to improve the specific immunoreactivity of antibody. The refolding procedure consists of consecutive dialysis baths with decreasing urea concentrations. Specificity and affinity constants were alternatively determined using ELISA and surface plasmon resonance, respectively.

Xenograft and chemotherapy

Animal studies were performed in accordance with protocols approved by the Institutional Animal Care and Use Committee (IACUC) of the University of Washington, according to the NIH guideline for laboratory animals. ICR *SCID* mice at an age of ~6 weeks were used. For tissue recombinants, fibroblasts and epithelial cells were admixed at a ratio of 1:4, with each recombinant comprised of 1.25×10^6 cells. Subrenal capsule implantation was performed, with animals killed 8 weeks after. Tumor volume (V) was determined per tumor length (l) and width (w): $V = (\pi/6) \times ((l+w)/2)^3$. For chemoresistance studies, mice received subrenal capsule xenografts under standard laboratory diets and water ad libitum for 2 weeks before administration of MIT (0.2 mg/kg doses) and/or anti-WNT16B (500 μl, 10 mg/kg doses) via i.p. injection on day 1 of week 3, 5 and 7. Totally 3 × 2-week cycles were administered. On completion of the regimen, kidneys were removed for tumor measurement and histological analysis. The cumulative MIT dose received per mouse was 0.6 mg/kg, anti-WNT16B 30 mg/kg. For systemic WNT16B induction by chemotherapy, MIT administration (i.v. infusion) followed the same schedule designed as above with the dose reduced to 0.1 mg/kg per injection (cumulative 0.3 mg/kg) to control overall toxicity. Through i.p. route, anti-WNT16B was given together with MIT, with the dose reduced to half correspondingly. At the end of 8th week, animals were killed with organs collected for examination.

ELISA assay

Serum levels of WNT16B and IL-8 from mice subject to chemotherapy and/or antibody treatment were quantified using ELISAs (MyBioSource, San Diego, CA, USA) according to manufacturer's instructions.

Statistics

All data are presented as the mean ± s.d. representative of at least triplicate experiments. For animal studies, no blinding was performed; $n = 10$ per group to ensure adequate power. The number of animals used gives an $\alpha = 0.05$, with power = 0.80. This analysis was based on data input from previous studies with PC3 tumors and responses to chemotherapeutic drugs.[4] Statistical analyses were performed on raw data for each group by one-way analysis of variance or a two-tailed Student's t-test, with $P < 0.05$ considered significant. The variance per assay was similar between the groups statistically compared.

CONFLICT OF INTEREST

The authors declare no conflict of interest.

ACKNOWLEDGEMENTS

We thank Dr Peter Nelson (Fred Hutchinson Cancer Research Center) for kindly providing fibroblast cell lines, essential reagents and conferring critical comments. This work was supported by a US DoD PCRP Idea Development Award (PC111703 to YS), the National Natural Science Foundation of China (81472709 to YS, 81272390 and 81472228 to JX) and the National 1000 Youth Elites Research Program of China (to YS).

REFERENCES

1 Klemm F, Joyce JA. Microenvironmental regulation of therapeutic response in cancer. *Trends Cell Biol* 2015; **25**: 198–213.
2 Sun Y. Translational horizons in the tumor microenvironment: harnessing breakthroughs and targeting cures. *Med Res Rev* 2015; **35**: 408–436.
3 Ostman A. The tumor microenvironment controls drug sensitivity. *Nat Med* 2012; **18**: 1332–1334.
4 Sun Y, Campisi J, Higano C, Beer TM, Porter P, Coleman I *et al.* Treatment-induced damage to the tumor microenvironment promotes prostate cancer therapy resistance through WNT16B. *Nat Med* 2012; **18**: 1359–1368.
5 Rodier F, Coppe JP, Patil CK, Hoeijmakers WA, Munoz DP, Raza SR *et al.* Persistent DNA damage signalling triggers senescence-associated inflammatory cytokine secretion. *Nat Cell Biol* 2009; **11**: 973–979.
6 Anastas JN, Moon RT. WNT signalling pathways as therapeutic targets in cancer. *Nat Rev Cancer* 2013; **13**: 11–26.
7 Huber RM, Lucas JM, Gomez-Sarosi LA, Coleman I, Zhao S, Coleman R *et al.* DNA damage induces GDNF secretion in the tumor microenvironment with paracrine effects promoting prostate cancer treatment resistance. *Oncotarget* 2014; **6**: 2134–2147.
8 Siamakpour-Reihani S, Caster J, Bandhu Nepal D, Courtwright A, Hilliard E, Usary J *et al.* The role of calcineurin/NFAT in SFRP2 induced angiogenesis--a rationale for breast cancer treatment with the calcineurin inhibitor tacrolimus. *PloS One* 2011; **6**: e20412.
9 Zhang S, Zhao W. Tumor microenvironment in pathogenesis and drug resistance of non-Hodgkin's lymphoma. *Zhonghua Xue Ye Xue Za Zhi* 2014; **35**: 466–469.
10 Borriello L, DeClerck YA. Tumor microenvironment and therapeutic resistance process. *Med Sci* 2014; **30**: 445–451.
11 Kinugasa Y, Matsui T, Takakura N. CD44 expressed on cancer-associated fibroblasts is a functional molecule supporting the stemness and drug resistance of malignant cancer cells in the tumor microenvironment. *Stem Cells* 2014; **32**: 145–156.
12 Seruga B, Ocana A, Tannock IF. Drug resistance in metastatic castration-resistant prostate cancer. *Nat Rev Clin Oncol* 2011; **8**: 12–23.
13 Basch E, Loblaw DA, Oliver TK, Carducci M, Chen RC, Frame JN *et al.* systemic therapy in men with metastatic castration-resistant prostate cancer: American Society of Clinical Oncology and Cancer Care Ontario Clinical Practice Guideline. *J Clin Oncol* 2014; **32**: U3436–U3133.
14 Halabi S, Lin CY, Small EJ, Armstrong AJ, Kaplan EB, Petrylak D *et al.* Prognostic model predicting metastatic castration-resistant prostate cancer survival in men treated with second-line chemotherapy. *J Natl Cancer Inst* 2013; **105**: 1729–1737.
15 Courtwright A, Siamakpour-Reihani S, Arbiser JL, Banet N, Hilliard E, Fried L *et al.* Secreted frizzle-related protein 2 stimulates angiogenesis via a calcineurin/NFAT signaling pathway. *Cancer Res* 2009; **69**: 4621–4628.
16 Sun Y, Nelson PS. Molecular pathways: involving microenvironment damage responses in cancer therapy resistance. *Clin Cancer Res* 2012; **18**: 4019–4025.
17 Coppe JP, Patil CK, Rodier F, Sun Y, Munoz DP, Goldstein J *et al.* Senescence-associated secretory phenotypes reveal cell-nonautonomous functions of oncogenic RAS and the p53 tumor suppressor. *PLoS Biol* 2008; **6**: 2853–2868.
18 Laberge RM, Zhou L, Sarantos MR, Rodier F, Freund A, de Keizer PL *et al.* Glucocorticoids suppress selected components of the senescence-associated secretory phenotype. *Aging Cell* 2012; **11**: 569–578.
19 Kongkham PN, Northcott PA, Croul SE, Smith CA, Taylor MD, Rutka JT. The SFRP family of WNT inhibitors function as novel tumor suppressor genes epigenetically silenced in medulloblastoma. *Oncogene* 2010; **29**: 3017–3024.

20 Saini S, Majid S, Dahiya R. The complex roles of Wnt antagonists in RCC. *Nat Rev Urol* 2011; **8**: 690–699.
21 Roth W, Wild-Bode C, Platten M, Grimmel C, Melkonyan HS, Dichgans J *et al.* Secreted Frizzled-related proteins inhibit motility and promote growth of human malignant glioma cells. *Oncogene* 2000; **19**: 4210–4220.
22 Paget S. The distribution of secondary growths in cancer of the breast. 1889. *Cancer Metastasis Rev* 1989; **8**: 98–101.
23 Ren SY, Johnson BG, Kida Y, Ip C, Davidson KC, Lin SL *et al.* LRP-6 is a coreceptor for multiple fibrogenic signaling pathways in pericytes and myofibroblasts that are inhibited by DKK-1. *Proc Natl Acad Sci USA* 2013; **110**: 1440–1445.
24 Cheng ZH, Biechele T, Wei ZY, Morrone S, Moon RT, Wang LG *et al.* Crystal structures of the extracellular domain of LRP6 and its complex with DKK1. *Nat Struct Mol Biol* 2011; **18**: 1204–U1244.
25 Bao J, Zheng JJ, Wu DQ. The Structural Basis of DKK-Mediated Inhibition of Wnt/LRP Signaling. *Sci Signal* 2012; **5**: pe22.
26 Asangani IA, Dommeti VL, Wang XJ, Malik R, Cieslik M, Yang RD *et al.* Therapeutic targeting of BET bromodomain proteins in castration-resistant prostate cancer. *Nature* 2014; **510**: 278–282.
27 Chen F, Qi X, Qian M, Dai Y, Sun Y. Tackling the tumor microenvironment: what challenge does it pose to anticancer therapies? *Protein Cell* 2014; **5**: 816–826.
28 Straussman R, Morikawa T, Shee K, Barzily-Rokni M, Qian ZR, Du JY *et al.* Tumour micro-environment elicits innate resistance to RAF inhibitors through HGF secretion. *Nature* 2012; **487**: 500–504.
29 Wilson TR, Fridlyand J, Yan YB, Penuel E, Burton L, Chan E *et al.* Widespread potential for growth-factor-driven resistance to anticancer kinase inhibitors. *Nature* 2012; **487**: 505–509.
30 Holohan C, Van Schaeybroeck S, Longley DB, Johnston PG. Cancer drug resistance: an evolving paradigm. *Nat Rev Cancer* 2013; **13**: 714–726.
31 Yang Y, Shi J, Gu Z, Salama ME, Das S, Wendlandt E *et al.* Bruton tyrosine kinase is a therapeutic target in stem-like cells from multiple myeloma. *Cancer Res* 2015; **75**: 594–604.
32 Vidal SJ, Rodriguez-Bravo V, Galsky M, Cordon-Cardo C, Domingo-Domenech J. Targeting cancer stem cells to suppress acquired chemotherapy resistance. *Oncogene* 2014; **33**: 4451–4463.
33 Corso S, Giordano S. Cell-autonomous and non-cell-autonomous mechanisms of HGF/MET-driven resistance to targeted therapies: from basic research to a clinical perspective. *Cancer Discov* 2013; **3**: 978–992.
34 Chen F, Zhuang X, Lin L, Yu P, Wang Y, Shi Y *et al.* New horizons in tumor microenvironment biology: challenges and opportunities. *BMC Med* 2015; **13**: 278.
35 Binet R. WNT16B is a new marker of cellular senescence that regulates p53 activity and the phosphoinositide 3-kinase/AKT pathway. *Cancer Res* 2009; **69**: 9183–9191.
36 von Marschall Z, Fisher LW. Secreted Frizzled-related protein-2 (sFRP2) augments canonical Wnt3a-induced signaling. *Biochem Biophys Res Commun* 2010; **400**: 299–304.
37 Mii Y, Taira M. Secreted Frizzled-related proteins enhance the diffusion of Wnt ligands and expand their signalling range. *Development* 2009; **136**: 4083–4088.
38 Bao J, Zheng JJ, Wu D. The structural basis of DKK-mediated inhibition of Wnt/LRP signaling. *Sci Signal* 2012; **5**: pe22.
39 Pazolli E, Alspach E, Milczarek A, Prior J, Piwnica-Worms D, Stewart SA. Chromatin remodeling underlies the senescence-associated secretory phenotype of tumor stromal fibroblasts that supports cancer progression. *Cancer Res* 2012; **72**: 2251–2261.
40 Chien Y, Scuoppo C, Wang X, Fang X, Balgley B, Bolden JE *et al.* Control of the senescence-associated secretory phenotype by NF-kappaB promotes senescence and enhances chemosensitivity. *Genes Dev* 2011; **25**: 2125–2136.
41 Orjalo AV, Bhaumik D, Gengler BK, Scott GK, Campisi J. Cell surface-bound IL--1alpha is an upstream regulator of the senescence-associated IL-6/IL-8 cytokine network. *Proc Natl Acad Sci USA* 2009; **106**: 17031–17036.
42 Alspach E, Flanagan KC, Luo X, Ruhland MK, Huang H, Pazolli E *et al.* p38MAPK plays a crucial role in stromal-mediated tumorigenesis. *Cancer Discov* 2014; **4**: 716–729.
43 Tsuchimochi K, Otero M, Dragomir CL, Plumb DA, Zerbini LF, Libermann TA *et al.* GADD45beta enhances Col10a1 transcription via the MTK1/MKK3/6/p38 axis and activation of C/EBPbeta-TAD4 in terminally differentiating chondrocytes. *J Biol Chem* 2010; **285**: 8395–8407.
44 Laberge L, Sun Y, Orjalo AV, Patil CK, Freund A, Liu S *et al.* mTOR regulates the tumor-promoting senescence-associated secretory phenotype. *Nat Cell Biol* 2015; **17**: 1049–1061.
45 Perry AS, O'Hurley G, Raheem OA, Brennan K, Wong S, O'Grady A *et al.* Gene expression and epigenetic discovery screen reveal methylation of SFRP2 in prostate cancer. *Int J Cancer* 2013; **132**: 1771–1780.
46 O'Hurley G, Perry AS, O'Grady A, Loftus B, Smyth P, O'Leary JJ *et al.* The role of secreted frizzled-related protein 2 expression in prostate cancer. *Histopathology* 2011; **59**: 1240–1248.
47 Yang X, Zhang X, Fu ML, Weichselbaum RR, Gajewski TF, Guo Y *et al.* Targeting the tumor microenvironment with interferon-beta bridges innate and adaptive immune responses. *Cancer Cell* 2014; **25**: 37–48.
48 Ries CH, Cannarile MA, Hoves S, Benz J, Wartha K, Runza V *et al.* Targeting tumor-associated macrophages with anti-CSF-1R antibody reveals a strategy for cancer therapy. *Cancer Cell* 2014; **25**: 846–859.
49 Sun Y. Tumor microenvironment and cancer therapy resistance. *Cancer Lett* 2015; e-pub ahead of print 10 August 2015; doi: 10.1016/j.canlet.2015.07.044.
50 Xu J, Zhong Y, Weixin N, Xinyu Q, Yanhan L, Li R *et al.* Preoperative hepatic and regional arterial chemotherapy in the prevention of liver metastasis after colorectal cancer surgery. *Ann Surg* 2007; **245**: 583–590.

Supplementary Information accompanies this paper on the Oncogene website (http://www.nature.com/onc)